EPR and ENDOR spectroscopic study of the reactions of aromatic azides with gallium trichloride†

Giorgio Bencivenni,[a] Riccardo Cesari,[a] Daniele Nanni,[a] Hassane El Mkami[b] and John C. Walton*[c]

Received 5th May 2010, Accepted 20th July 2010
DOI: 10.1039/c0ob00084a

The reactions of gallium trichloride with phenyl and deuterio-phenyl azides, as well as with 4-methoxyphenyl azide and deuterium isotopomers, were examined by product analysis, CW EPR spectroscopy and pulsed ENDOR spectroscopy. The products included the corresponding anilines together with 4-aminodiphenylamine type dimers, and polyanilines. Complex CW EPR spectra of the radical cations of the dimers $[ArNHC_6H_4NH_2]^{+\bullet}$ and trimers $[ArNHC_6H_4NHC_6H_4NH_2]^{+\bullet}$ were obtained. These EPR spectra were analysed with the help of data from the deuterium-substituted analogues as well as the pulse Davies ENDOR spectra. DFT computations of the radical cations provided corroborating evidence and suggested the unpaired electrons were accommodated in extensive π-delocalised orbitals. A mechanism to account for the reductive conversion of aromatic azides to the corresponding anilines and thence to the dimers and trimers is proposed.

Introduction

Many novel applications of organic azides in synthetic organic chemistry have been appearing in the literature in recent years.[1] One reason for this is the facility with which nitrogen-centred radicals can be generated from the azido group.[2] Alkyl, vinyl, aryl, and acyl radicals, for example, can ring close onto aliphatic and aromatic azides yielding five and/or six-membered cyclic aminyl radicals, which in turn are key intermediates for the construction of *N*-heterocycles.[3] Recently, azides have been shown to be useful intermediates for generation of iminyl radicals as well.[4] The realm of radical reactions in general, and of radical generation from azides in particular, has long been dominated by toxic metal reagents and, especially, organotin compounds. In the search for efficient purification procedures and sound tin substitutes the last years have witnessed thorough investigations of novel ways of carrying out radical reactions in the absence of tin reagents.[5] Concerning this, the use of indium derivatives (dichloroindium hydride in particular), as well as other Group 13 metal compounds,[6] including organogallium compounds,[6c,h,l] has come to the forefront of radical organic synthesis as a more benign alternative to other metal-based catalysts. This class of reagents has recently found applications in the field of azide radical chemistry as well, resulting in reduction of a variety of organic azides to the corresponding amines and cyclisation of γ-azidonitriles to pyrrolidin-2-imines with dichloroindium hydride.[7a] Allylated nitrogen heterocycles have been obtained by reaction of δ-azido esters and chlorides with allylindium dichloride.[7b] In the course of the latter studies, only indirect evidence of the intermediacy of nitrogen-centred radicals was obtained, including the EPR spectrum of the allyl radical during photolysis of allylindium dichloride.[7b] Any attempt to detect aminyl radicals by treatment of azides with indium (or other Group 13 metal) reagents failed, independently of the technique of generation of the initial metal-centred radicals. However, during one of those attempts, we realised that Group 13 metal halides, when treated with organic azides, gave rise to strong, persistent EPR signals that were particularly consistent in the case of gallium trichloride.[8] Here we report the results obtained from the reactions of some aromatic azides with gallium trichloride.

[a]*Dipartimento di Chimica Organica "A. Mangini", Università di Bologna, Viale del Risorgimento 4, I-40136 Bologna, Italy. E-mail: nanni@ms.fci.unibo.it*
[b]*School of Physics and Astronomy, University of St. Andrews, St. Andrews, Fife, UK, KY16 9SS. E-mail: hem2@st-andrews.ac.uk*
[c]*School of Chemistry, University of St. Andrews, EaStChem, St. Andrews, Fife, UK, KY16 9ST. E-mail: jcw@st-and.ac.uk; Fax: +44 (0)1334 463808; Tel: +44 (0)1334 463863*

† Electronic supplementary information (ESI) available: Details of preparations of isotopically substituted anilines. EPR spectra of deuterium substituted species from azides **8b–8e**. ENDOR simulations for species from azides **1a** and **1d**. Cartesian coordinates for DFT computed structures. See DOI: 10.1039/c0ob00084a

Results and discussion

Products from reactions of aryl azides with gallium trichloride

Gallium trichloride (0.25 mmol) in pentane (0.55 mL) was added to phenyl azide **1a** (0.25 mmol) in dichloromethane (4.0 mL) at room temperature. A vigorous reaction with gas evolution (probably nitrogen) was observed and the colour changed from pale yellow to dark green and eventually to deep violet. The solution was examined by 9 GHz EPR spectroscopy and found to exhibit strong and complex spectra that persisted for several weeks in the absence of oxygen. The resultant mixture was analysed by GC-MS, and the major products were isolated.

In this way it was shown that the mixture contained unreacted **1a** together with aniline (**2a**), 4- and 2-chloroanilines (**3a** and **4a**), 4-aminodiphenylamine (**5a**), plus traces of 2-aminodiphenylamine (**6a**) and 5,10-dihydrophenazine (**7a**) (Scheme 1).

The reaction was repeated with several sets of starting conditions and the product yields are set out in Table 1.

When the reaction was carried out with a 3-fold excess of $GaCl_3$ (entry 2) the starting azide was completely consumed and 4-chloroaniline (**3a**) was the almost exclusive product with only traces of **4a** and **5a**. This suggested $GaCl_3$ was involved in the

Table 1 Product yields from reaction of **1a** with $GaCl_3$[a]

Entry	**1a** : $GaCl_3$	Solvent	**1a**[b]	**2a**	**3a** & **4a**	**5a**
1	1 : 1	CH_2Cl_2 pentane	45	5	15 & 22	10
2	1 : 3	CH_2Cl_2 pentane	0	0	90 & t	t
3	3 : 1	CH_2Cl_2 pentane	nd	t	t & t	50
4[c]	1 : 1	CH_2Br_2 pentane	nd	30	25 & 15	20

[a] Yields in mol%. [b] Unreacted **1a**; t = trace, nd = not determined. [c] Traces of chlorinated 4-aminodiphenylamine were also observed.

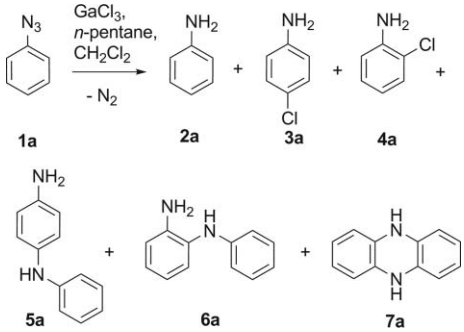

Scheme 1 Products from reaction of phenyl azide with gallium trichloride.

chlorination of aniline, probably by an electrophilic mechanism. When CH_2Br_2 was used in place of CH_2Cl_2 (entry 4) the products were again aniline and chloroanilines together with "dimer" **5a**. No bromoanilines were detected. This confirmed that the $GaCl_3$, rather than the CH_2Cl_2 solvent, was the source of the Cl atoms. When a 3-fold excess of azide was used (entry 3) only traces of aniline and chloroanilines were observed and the 'head to tail' dimer **5a** became the main product. Significant amounts of tars were also noted.

Literature research has shown that anilines can easily be oxidised to the corresponding resonance-stabilised radical cations, which can couple with more aniline to afford very persistent radical cation dimers.[9] It seemed possible, therefore, that the species we observed by EPR spectroscopy might be related to dimer **5a**. The generation of these radical cations depends critically on reaction conditions, in particular the degree of protonation, which can facilitate the electron transfer (ET).[10] It has also been reported that electrochemical oxidation of aromatic amines can generate the same radical cations which can polymerize giving oligo- and poly-anilines.[11]

4-Methoxyphenyl azide (**8a**) also reacted vigorously with $GaCl_3$ leading to evolution of nitrogen and formation of a deep blue colour.[12] The EPR spectra exhibited strong signals that persisted for many weeks. Product analyses demonstrated the reaction was less sensitive to reaction conditions and always furnished 4-amino-4′-methoxydiphenylamine (**9a**, *Variamine blue*) as the main product, together with traces of 4-methoxyaniline (**10a**), 4-(4-methoxyphenylamino)phenol (**11a**), its oxidised quinonic form **12a** (Scheme 2), 2,7-dimethoxy-5,10-dihydrophenazine and much dark coloured polymer.

The observation of **10a** suggested that this amine was again the precursor for the other products. Thus, **9a** might result from substitution on **10a** by a radical, or radical-cation related to **10a**, accompanied by loss of the methoxy group. Direct ESI-MS

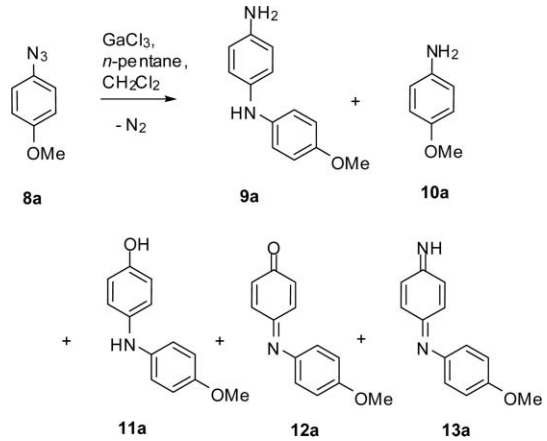

Scheme 2 Products from reaction of azide **8a** with gallium trichloride.

analysis of the total reaction mixture in positive ion mode showed a compound with mass 213 amu. This corresponds to protonated quinodiimine **13a**. It seems probable that a sequence of oxidations is responsible for the series **9a**, **13a**, **11a**, **12a**, possibly during work-up.[13] Analysis in negative ion mode showed a peak corresponding to $GaCl_4^-$, suggesting this was the counter-ion for the organic radical cations.[14]

Preparation of deuteriated and ^{15}N-substituted aromatic azides

As an aid to analyzing the complex EPR spectra, a series of deuterium-substituted phenyl azides (**1b–d**) and 4-methoxyphenyl azides (**8b–e**) was prepared as well as the ^{15}N-isotopomer **8f** (Scheme 3). Deuteriated azides **1b–d** and **8b–e** were prepared by standard diazotisation techniques starting from the previously reported deuteriated anilines; azide **8f** was synthesised from the known 4-methoxyaniline-^{15}N by diazo-transfer reaction with azido tris(diethylamino)phosphonium bromide (see Electronic Supplementary Information for details and references).

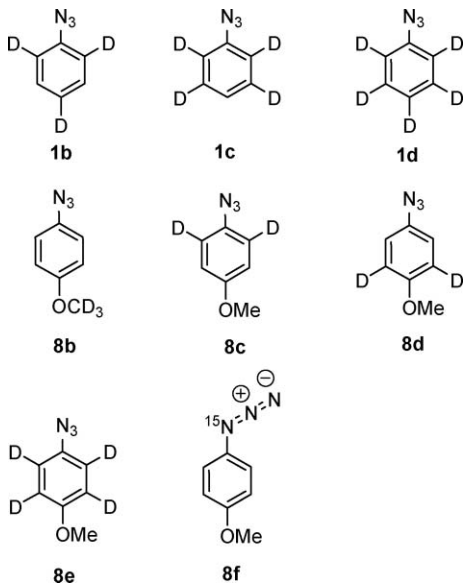

Scheme 3 The set of deuterium- and ^{15}N-substituted aromatic azides.

EPR spectroscopic study of intermediates from phenyl and deuterio-phenyl azides

The aromatic azides were reacted with $GaCl_3$ in CH_2Cl_2–pentane solution. Aliquots (*ca.* 0.1 mL) were placed in quartz capillary tubes (dia. 1 mm), purged with nitrogen for 15 min, and transferred to the resonant cavity of a 9 GHz EPR spectrometer. Strong spectra of persistent species were observed, but the pattern evolved with time and reaction conditions. A set of spectra obtained from PhN_3 is shown in Fig. 1.

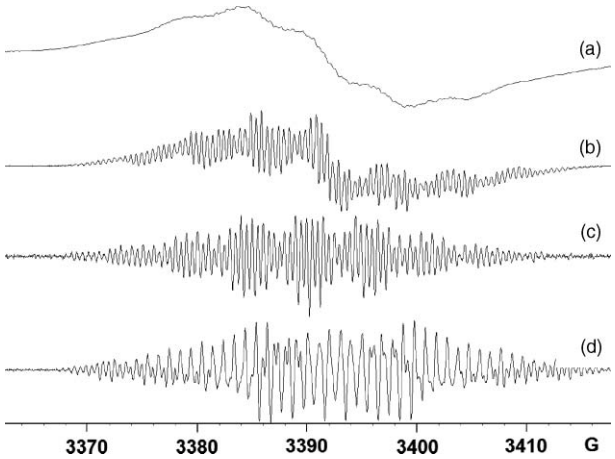

Fig. 1 EPR spectra from PhN_3 and $GaCl_3$. (a) 1st derivative spectrum on first mixing. (b) 1st derivative spectrum after several hours. (c) 2nd derivative of b [species (i)]. (d) 2nd derivative of another species (ii) in CD_2Cl_2 solution.

On first mixing the reactants, broad strong spectra (Fig. 1a) were usually obtained but over a matter of hours, or after irradiation with UV light, fine structure usually developed (Fig. 1b). A broad central component was always present and we attribute this to persistent polymeric and oligomeric paramagnetic species. By using 2nd derivative presentation with a low modulation amplitude (0.2 Gpp) discrimination against the broad component was achieved and a well resolved spectrum resulted (Fig. 1c). When CD_2Cl_2–pentane was used as solvent in place of CH_2Cl_2–pentane another spectrum, well resolved in 2nd derivative mode, was observed (Fig. 1d). The same spectrum as in (d) was also observed on occasion in CH_2Cl_2–pentane, during the evolution of the spectral pattern with time. The spectra shown in (c) and (d) clearly correspond to two *different* species (i) and (ii).

To assist in analyzing the spectra and identifying the paramagnetic species, the deuteriated azides **1b–d** were individually treated with $GaCl_3$ under the same conditions. The best resolved spectra, together with computer simulations, are shown in Fig. 2. As expected, the deuterium substitution caused some broadening of the spectra, but resolution was still satisfactory.

The spectrum from the fully deuteriated azide **1d** was well simulated by using three non-equivalent N-atom hyperfine splittings (hfs) and two equivalent H-atom hfs (Table 2). Similarly, the spectrum from the tetra-deuterio azide **1c** was well simulated with a quite similar set of hfs (Table 2). A good simulation of the spectrum from the tri-deuterio azide **1b** was obtained with again nearly the same three non-equivalent N-atom hfs, the same two equivalent H-atom hfs and additional hfs from four equivalent

Table 2 EPR parameters for paramagnetic "trimer" species **15** from **1a–d**[a,b]

Precursor azide	N-8	N-15	N-1	2 × H-1	H-8	H-15	H-rings
1a species (i)	5.0	4.9	3.0	6.5	4.9	2.1	2.1(3H) 1.0(3H)
1b	5.2	4.8	2.5	6.5	D[c]	D[c]	2.0(4H)
1c	5.4	5.0	2.9	6.4	D[c]	D[c]	—
1d	5.2	4.9	2.5	6.5	D[c]	D[c]	—
DFT[d] for **15a**	5.3	3.4	2.1	−3.0	−7.7	−4.8	−1.6(4H) −1.1(3H) −0.6(2H) 0.6(2H) −0.2(2H)

[a] Hfs in G; note that the experimental EPR spectra can only give the magnitude (not the sign) of hfs. [b] The atom numbers in line 1 are defined in Scheme 4. [c] Hfs from D-atoms not resolved. [d] UB3LYP/6-31G(d).

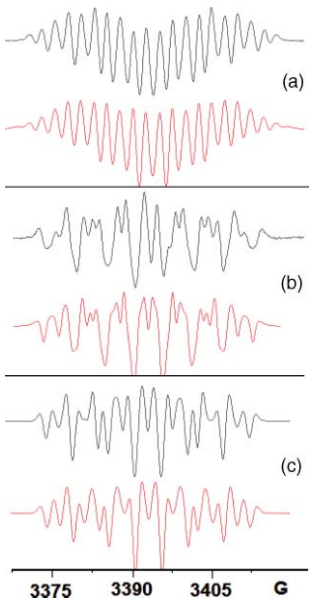

Fig. 2 2nd Derivative EPR spectra from **1b–1d** and $GaCl_3$ at 300 K in DCM–pentane. Top: (a) Spectrum from **1b**: upper, experimental; lower, simulation. Centre: (b) Spectrum from **1c**: upper, experimental; lower, simulation. Bottom: (c) Spectrum from **1d**: upper, experimental; lower, simulation.

H-atoms (Table 2 and Fig. 2). Although the simulations were not unique, and satisfactory computer simulations could be obtained for individual spectra with other sets of parameters, the data of Table 2 and Fig. 2 was the only global set that gave a consistent picture for all three isotopically substituted species.

By utilising the three N-atom and two equivalent H-atom hfs derived from the deuterium-substituted species we were able to obtain a satisfactory simulation of species (i) derived from the parent azide **1a** (Fig. 3a). The good quality of the agreement is shown in Fig. 3 and the corresponding hfs are noted in Table 2.

A different set of parameters was required for the analysis of the spectrum of species (ii). In this case good fits were only obtained with two equivalent N-atoms, three sizeable H-atom hfs and several additional ring H-atom hfs (Fig. 3 and Table 3).

The hfs we observed for species (ii) are quite similar to those reported in the literature for the radical cation of 4-aminodiphenylamine (**14a**)[9b,15] (Table 3). The small differences

Table 3 EPR parameters for dimer species (ii) from **1a**[a]

	N-8, N-1	H-8	2 × H-1	H-14, 5	H-6, 10	H-11, 13,3	H-4, 12
Exptl.	4.9,4.9	6.8	5.6	3.1	2.0	1.0	0.6
Lit. for **14a**[b]	5.4,4.9	6.6	6.0	1.7	1.7	1.1	0.6
DFT[c]	6.1,3.8	−8.7	−5.7	−2.6, −2.2	−2.1, −2.0	−1.9,1.2, −1.1	−1.1, 1.0
DFT[d]	2.6,3.1	−4.8	−5.7	−2.6, −2.1	−2.3, −2.1	−0.8, −0.1, −1.8	−2.3, −0.9

[a] hfs in G; note that the experimental EPR spectra can only provide the magnitude (not the sign) of hfs. The atom numbers in line 1 are defined in Scheme 4. [b] See ref. 9, 15. [c] UB3LYP/6-31G(d). [d] UB3LYP/epr-iii (see ref. 19).

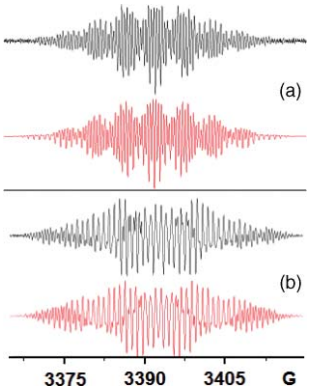

Fig. 3 Experimental and simulated EPR spectra from PhN_3 and $GaCl_3$ at 300 K. Top panel (a): 2nd derivative experimental and simulated spectra of species (i). Bottom panel (b): 2nd derivative experimental and simulated spectra of species (ii).

are probably due to the different solvent and counter ions. In view of our observation of the amine **5a** as a major product, we can confidently identify species (ii) as radical cation **14a**. On the other hand, species (i) from **1a**, and all the paramagnetic species from the deuteriated azides **1b–d**, showed the presence of 3 non-equivalent N-atoms. The most probable explanation is that these signals correspond to the "trimer" **15a** [*N*1-(4-aminophenyl)-*N*4-phenylbenzene-1,4-diamine] and deuterium isotopomers thereof **15x–z** (Scheme 4).

In the case of **15a**, derived from the parent azide, the hfs from all three N-atoms were resolved, as well as the hfs from the amino H-atoms. Hfs from six of the total thirteen ring H-atoms were also resolved. The DFT computation (Table 2) was in reasonable agreement and suggested that at least six of the ring H-atoms would be too small to be resolved. In agreement with our analysis, the trimer cations **15y** and **15z** showed no resolved hfs from their almost fully deuteriated rings. The spectral data established that for both **15y** and **15z** the terminal NH_2 groups contained H-atoms rather than D-atoms. Interestingly, however, in both cases, the chain amino groups (N-8, N-15) gave no resolved hfs, and therefore they were present as ND groups. In the case of **15x**, derived from the 2,4,6-trideuterio-azide **1b**, a similar picture emerged, except that hfs from four of the ring positions were now resolved. Thus, the EPR spectra suggested an evolution in the $GaCl_3$ promoted reaction of phenyl azide from the long-lived radical cation of 4-aminodiphenylamine (the dimer), to a long-lived trimer radical cation, and thence to long-lived oligomeric and polymeric species with broad EPR spectra.

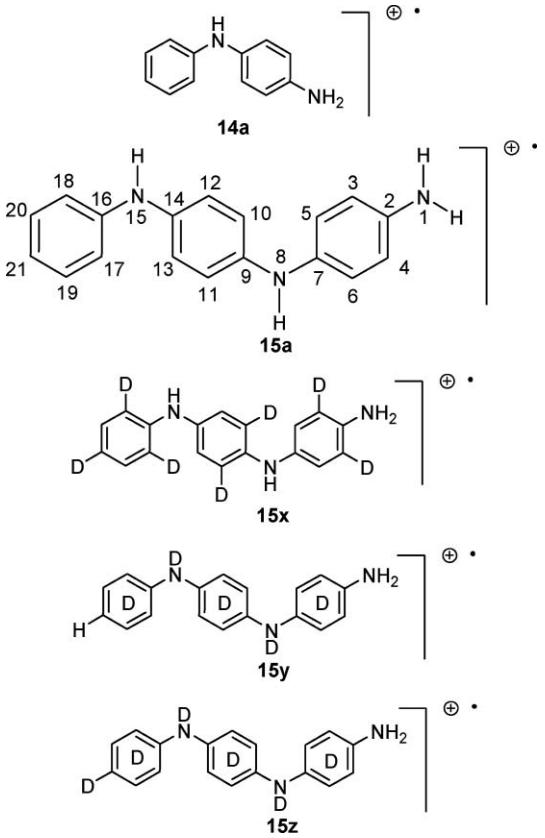

Scheme 4 Radical cations derived from phenyl azide.

EPR spectra of intermediates from 4-methoxyphenyl azide, deuteriated analogues and ^{15}N-substituted azide 8f

The 4-methoxyphenyl azides **8a–f** were reacted individually at room temperature with $GaCl_3$ in CH_2Cl_2–pentane solution in the same way as the phenyl azides. The reactions followed a similar course in that nitrogen was evolved and deep blue colours (sometimes appearing green) developed along with much dark polymer. The EPR spectra showed strong and very persistent signals which were initially broad, somewhat like the top spectrum (a) in Fig. 1, but which developed fine structure on standing. All the spectra contained broad central components which were discriminated against by use of low modulation intensities. Final traces of the broad components were digitally removed. The spectrum from **8a** and its ^{15}N-isotopomer **8f** are shown in Fig. 4. Spectra from deuteriated azides **8b–e** are in the ESI.

Computer simulations were non-trivial because of the multiplicity of lines and because small differences in line width, as well as

Table 4 EPR data from 4-amino-4′-methoxydiphenylamine radical cations **14** derived from 4-$MeOC_6H_nD_{4-n}{}^xNN_2$ and $GaCl_3$[a]

Precursor azide [H or D]	N-8	N-1	H-8	2H-1	2H/2D-5,6	2H/2D-10,11	2H-3,4	2H-12,13
8a [H_4]	5.2	4.4	7.3	3.8	3.1	2.2	0.8	0.4
DFT for **14c**[b]	6.1	3.1	–8.7	–4.6	–2.8	–2.1	–0.7	0.4
8f [H_4,^{15}N]	7.4 (^{15}N)	6.1 (^{15}N)	7.4	3.8	3.0	2.2	0.8	0.4
8b [OCD_3]	5.2	4.3	7.3	3.9	3.1	2.2	0.8	—
8c [D_2]	5.3	4.1	7.0	3.6	0.5 (2D)	0.5 (2D)	0.8	—
8d [D_2]	5.3	3.8	1.3 (D)	4.0	3.0	2.3	—	—
8e [D_4]	5.2	4.4	7.1	3.6	0.66 (2D)	0.55 (2D)	—	—

[a] Hfs in G for CH_2Cl_2–pentane soln. at 300 K. Atom numbers in column headings refer to the positions defined in structure **15a**. [b] DFT computation for radical cation **14c** using UB3LYP/6-31G(d).

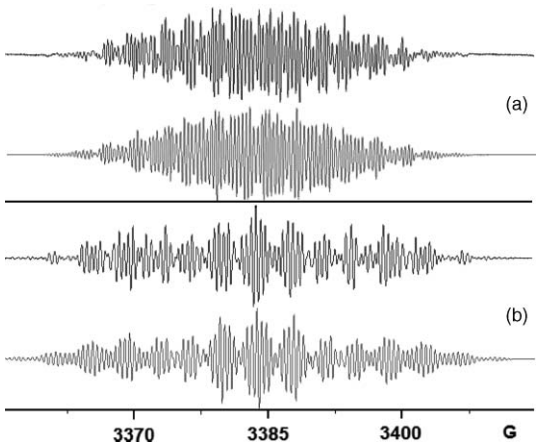

Fig. 4 EPR spectra from 4-methoxyphenyl azides. Top panel (a): Experimental EPR spectrum from **8a** in CH_2Cl_2–pentane at 300 K with the computer simulation below. Bottom panel (b): Experimental EPR spectrum from ^{15}N- isotopomer **8f** with the simulation below.

in the hfs, had a large effect on the appearance of the spectra. The spectra of the deuterium-substituted species were well resolved and this, together with the good spectrum from **8f**, enabled a complete analysis to be carried out. The derived hfs are listed in Table 4.

The hfs form a very consistent set and the magnitudes of both N-hfs and H-hfs are conserved from one species to another as would be expected for D- and ^{15}N-substitution. The ratio of the nuclear magnetic moments $^{14}N/^{15}N$ is 1.4 so the $a(^{14}N)$ values calculated from the $a(^{15}N)$ values (Table 4, line 4) are 5.3 and 4.4 G; in close agreement with the observed $a(^{14}N)$ values from **8a** (Table 4, line 2).

Similarly the ratio $[\mu_D/I_D]]/[I_H/\mu_H]$ is 6.5 giving calculated a(2D)-5,6 and a(2D)-10,11 values of 0.55 and 0.3 G respectively. These are in satisfactory agreement with the data in Table 4 (lines 5, 6) taking into account the fact that the line widths of 0.1 to 0.2 G introduced error limits of this order. Interaction of the unpaired electron with the 4-CH_3O group was too small for CH_3 hfs to be resolved. The spectrum of the species from **8a** was, therefore, almost identical to that from the CD_3O-analogue **8b** (compare Table 4, line 2 with line 5). The overall analysis of Table 4 shows that a single paramagnetic species containing 2 non-equivalent N-atoms, 3 (N)-H atoms and 8 H/D-atoms was responsible for all the spectra. There can be little doubt that this is the radical cation of 4-amino-4′-methoxydiphenylamine (**9a**, *Variamine blue*). A DFT computation on **14a** [UB3LYP/6-31G(d)] gave hfs in satisfactory agreement (Table 4, line 3). No "trimer" radical cations, analogous to **15**, were observed in any of the experiments. Previously reported EPR spectra of the *Variamine blue* radical cation were not well resolved and hence the derived hfs [a(2 N) = 5.6, a(3H) = 7.6, a(4H) = 2.0 G at rt in water] were approximate estimates.[16] The reasonable correspondence between these values and those of Table 4 supports our identification.

One difference between the spectra obtained from the deuterium-substituted versions of the "trimer" radical cations, that is **15b–d**, and the deuterium isotopomers of **14** was that the latter were better resolved with smaller line widths [compare Fig. 4 (and the examples in the ESI) with Fig. 2]. The probable reason was that in the deuterium isotopomers of **14** all the amino groups remained as NH or NH_2 (Table 4) whereas in **15y–z** the chain amino groups appeared as ND. The presence of 2 non-equivalent, exchangeable, ND atoms, with comparatively large unresolved, a(D) values, probably accounts for the somewhat broader lines of the **15y–z** spectra in Fig. 2. One exception to this was the spectrum of **14d** from **8d** (see ESI) which did have broader lines. The simulations suggested that the central NH group had become ND in this case, although slightly better fits were obtained by adding in *ca.* 30% of the species retaining NH. The assignments of the hfs to particular atoms in Table 4 are, of course, tentative: the DFT computed values were used as a guide.

Pulse ENDOR spectra of intermediates from 1a and tetra-deuteriophenyl azide 1c

In seeking support for our identifications of the intermediates, pulsed ENDOR experiments, based on the ESE effect, were carried out on the frozen solutions from azides **1a** and **1c**. The echo signal was created by the microwave pulse sequence and an rf pulse was applied during the "mixing period" which corresponded to the time T in the Davies ENDOR sequence. The rf pulse drove the nuclear spin transitions which led to a change in the ESE intensity. The ENDOR signal was therefore measured by monitoring the ESE intensity while the rf frequency was varied. In the case of an $S = \frac{1}{2}$ system coupled with a nucleus with nuclear spin $I = \frac{1}{2}$, the Davies ENDOR spectrum consists of two lines at the nuclear resonance frequencies ν_α and ν_β which correspond to the transitions associated to the electron spin manifold $M_s = +\frac{1}{2}$ and $M_s = -\frac{1}{2}$ respectively. If the Larmor frequency (ν_n) of the nucleus in question is larger than the hyperfine interaction then the resonance frequencies are given by: $\nu_{\alpha\beta} = |\nu_n \pm \frac{1}{2}a_{iso}|$; if ν_n is less than $a_{iso}/2$ the frequencies are then given by: $\nu_{\alpha\beta} = |\frac{1}{2}a_{iso} \pm \nu_n|$. The presence of anisotropy considerably alters this picture, and a_{iso} is replaced

by A_i (*i.e.*, one of the principal components of the hyperfine tensor) to take account all the orientations of the molecule with respect to the applied magnetic field.

In Fig. 5, we report the Davies ENDOR spectrum from the species derived from the **1a** sample at 50 K. The inset shows the ESE-EPR spectrum, with the arrow indicating the magnetic field position at which the ENDOR experiment was performed. The ENDOR spectra show powder pattern lineshapes, as expected for frozen solutions, due to the anisotropic hyperfine interactions.

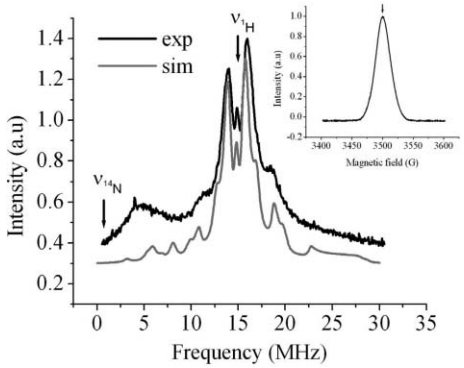

Fig. 5 Davies ENDOR spectrum of species (**14a**) from **1a** at 50 K.

Two main features cover the whole spectrum; a powder pattern centred about the ^{1}H Larmor frequency and a second broad signal located at lower frequency and spread over 8 MHz width. A well-marked singlet appears at the centre of the ^{1}H pattern due to very small, unresolved coupling corresponding to interaction of the unpaired electron with the matrix and probably to the presence of polymer radical cations. The ENDOR spectrum of the species from **1a** appears somewhat asymmetric which could be related to the saturation of the nuclear transition in one of the electron spin manifolds.[17]

The ENDOR spectrum of the species from **1c** is shown in Fig. 6. This contains a powder pattern centred about the ^{1}H Larmor frequency, again with a strong central singlet, together with a broad signal at lower frequency and an additional well resolved doublet with a splitting of 0.94 MHz centred around the ^{2}H (D) Larmor frequency.

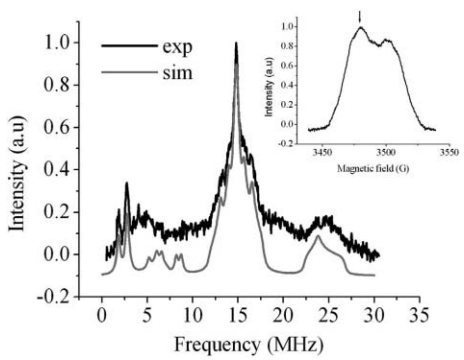

Fig. 6 Davies ENDOR spectrum of species (**15y**) obtained from deuteriated azide **1c** at 50 K.

The lack of resolution encountered in these ENDOR spectra makes a direct assignment of these signals to the different nuclei difficult. Therefore, to interpret the ENDOR data, our ENDOR simulations were based mainly on the CW EPR results. The simulated spectra are displayed in Fig. 5 & 6.

A decomposition of each simulation into the contributions from individual magnetic nuclei is given in the ESI. The ENDOR simulation tensors are also given in the ESI. Each ^{1}H contributes three sets of peaks to the spectrum times the number of ^{1}H's present. This represents an enormous number of lines in one spectrum. Obviously they cannot all be assigned from this broad unresolved powder pattern. Almost axial tensors were assumed (see ESI). However, it should be noted that it may well be possible to simulate these spectra with other parameter sets. The experimental Davies ENDOR data supports the CW EPR data in confirming the magnitudes of the hyperfine couplings and the nitrogen interactions.

There were some differences in the case of the deuteriated trimer **15y**. Only one D coupling of *ca.* 0.3 G was resolved. This is close to the value expected for (N)D-15 (see Table 2). A second D hyperfine from (N)D-8 (*ca.* 0.8 G based on the H-8 value) was expected. However, these amino D/H atoms are readily exchangeable and it is probable that (N)D-8 exchanged for (N)H-8 in the sample studied by ENDOR. This sample was several days older than the CW EPR sample. The region of Fig. 6 centred around the ^{1}H Larmor frequency also shows more couplings than expected for **15y** which has only 2 types of ^{1}H. However the additional couplings can also be attributed to H/D exchange.

DFT computations on radical cations

Quantum chemical calculations were carried out with the Gaussian 03 programme package.[18,19] Density functional theory with the UB3LYP functional, was employed. The equilibrium geometries were fully optimised with respect to all geometric variables, no symmetry being assumed, with the 6-31G(d) basis set. Computed $<S^2>$ values for the radical cations were 0.7500 after annihilation of higher multiplicity spin states. Isotropic EPR hfs were derived from computed Fermi contact integrals evaluated at the H- and N-nuclei. The hfs were taken directly from the Gaussian output files.

The optimum structures of the radical cations **14a** and **15a**, and their associated SOMOs, are shown in Fig. 7.

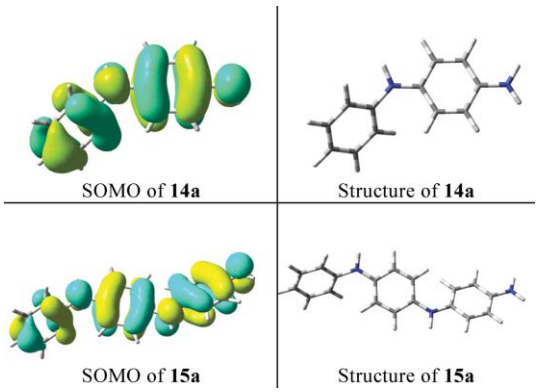

Fig. 7 DFT computed structures and SOMOs for dimer and trimer radical cations.

The C–NH_2 bond lengths in radical cation **14a** (1.35 Å) and **15a** (1.36 Å) indicated significant double bond character, as did the central C–NH bond lengths which were all ≤ 1.415 Å. The CNC angle in **14a** was 130.3° and the CNC angles in **15a** were 130.8 and 129.5° for 7-8-9 and 14-15-16 respectively, showing significant widening from trigonal. The aromatic rings in both structures twisted significantly out of co-planarity. It seems that a compromise was reached in which the repulsive steric interaction between *ortho*-H-atoms of neighbouring rings was balanced against the stabilising effect from conjugation of the π-systems. The SOMOs depicted in Fig. 7 show that there was still sufficient orbital overlap to support lengthy π-systems extending over all the rings and N-atoms in both structures. This is in good accord with the EPR spectroscopic data which shows extensive delocalisation of the unpaired electron. The computed hfs are in Tables 2 and 3 and they show reasonable correspondence with experiment.

Conclusions

Aniline **2a** and 4-chloroaniline **3a** as well as 4-aminodiphenyl amine **5a** were major products from the reaction of **1a**. Similarly, azide **8a** gave the corresponding aniline **10a** and dimer **9a**. It is probable that the chloroanilines were formed by an electrophilic substitution on aniline in which $GaCl_3$ acted as Lewis acid *and* supplied the chlorine atoms. The presence of the chloroanilines and the rapid evolution of N_2 suggested that aniline and 4-methoxyaniline were formed early in the respective reactions. Literature reports have indicated that anilines can be converted to 4-aminodiaryl amines (the dimers) under various oxidative conditions.[9b,11,15] Mechanisms suggested for dimer formation from anilines include:[20] (i) initial formation of the radical cation $ArNH_2^{+\bullet}$ which then couples with more aniline and forms the 4-aminodiaryl amine radical cation after loss of HX, (ii) formation of the aniline radical $ArNH^{\bullet}$ which couples with $ArNH_3^+$, $ArNH_2$, or $ArNH_2^{+\bullet}$. A possible mechanism for production of the anilines is shown in Scheme 5. Coordination of the $GaCl_3$ to **1a** or **8a** will give rise to an adduct **17** that can be reduced by more azide to give, after nitrogen loss, a gallium-coordinated aminyl radical **18**. The H-atom source is probably mainly solvent (SH), rather than the aromatic rings, because even the fully deuteriated precursor **1d** gave intermediate radical cations containing H-atoms. Thus **18** picks up an H-atom to produce **19** which will protonate to yield the aniline [**2a**, **3a** or **10a**] and $GaCl_4^-$.

There are several potential routes to the dimer radical cations. Radical **18** might add to the aniline with production of delocalised radical **21**. Elimination of $GaCl_3X^-$ would then yield radical **22** which on protonation would afford the observed long-lived dimer radical cations **14**. Of course, proton transfer could occur earlier in the reaction, such that coupling takes place with the anilinium cation instead. The presence of much 4-chloroaniline in the reaction with **1a** means that coupling with **18** could take place with **3a** as well as **2a** so there is potential in this system for formation of both the 4-aminodiphenyl amine radical cation **14a** and *N*1-(4-chlorophenyl)benzene-1,4-diamine **14b** and/or the corresponding trimers **15a,b**. The EPR spectrum of species (ii) from **1a** showed unequivocally that **14a** with no Cl substituent was formed (see Table 3). However, in the case of the trimer radical cations **15a,x–z**, hfs were not observable from all sites so the presence of a Cl-substituent cannot be ruled out. Trimerisation was evidently easier for the PhN_3 system than the 4-MeO-analogue. This might be because elimination of Cl^- to afford **22** takes place more easily than elimination of MeO^-. Two such eliminations are needed for the formation of **15**.

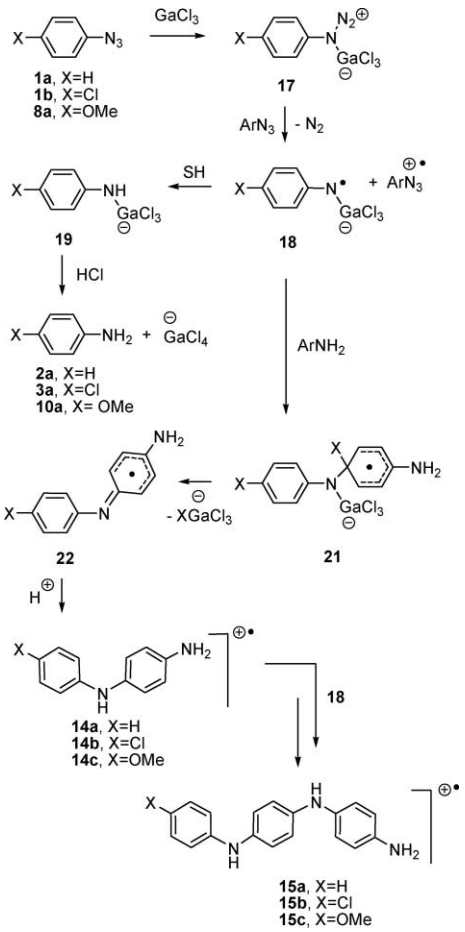

Scheme 5 Mechanism of reductive formation of anilines, dimers and trimers from aromatic azides.

We have shown that two aromatic azides react with gallium trichloride in hydrocarbon solvents to yield deeply coloured solutions of very persistent radical cations. Well-resolved EPR spectra of these species were eventually obtained and analysed. The experimental isotropic hfs, coupled with DFT computations, showed these were radical cations of the dimer 4-aminodiphenylamine and trimer (*N*1-(4-aminophenyl)-*N*4-phenylbenzene-1,4-diamine) and these species were comprehensively characterised. ENDOR spectra of the frozen solutions provided supporting information. It appears that the $GaCl_3$ promoted reactions of azides resemble those of aromatic amines under oxidative conditions. In CH_2Cl_2–pentane solvent the conditions are just right for initial conversion of the azides to anilines which then couple to give dimers, trimers and, eventually, polyanilines.

Experimental

EPR and ENDOR spectroscopy

EPR spectra were obtained with a Bruker EMX 10/12 spectrometer fitted with a rectangular ER4122 SP resonant cavity and operating at 9.5 GHz with 100 kHz modulation. An aliquot (*ca.*

0.1 mL) of the reaction mixture from each aromatic azide and $GaCl_3$ in CH_2Cl_2–pentane solution was placed in a 1 mm o.d. quartz capillary tube, de-aerated by bubbling nitrogen for 20 min and transferred to the resonant cavity. Spectra were examined at several temperatures but generally best resolution and signal intensity were obtained at around 300 K. Most of the EPR spectra were recorded with 2.0 mW power, 1.0 to 0.2 G_{pp} modulation intensity and a gain of *ca.* 10^6. In all cases where spectra were obtained, hfs were assigned with the aid of computer simulations using the Bruker SimFonia and NIEHS Winsim2002 software packages.

Pulsed EPR and ENDOR were performed using a pulsed EPR spectrometer (Bruker Elexsys E580) equipped with a Dice-ENDOR accessory, a radio frequency (rf) amplifier and a dielectric-ring ENDOR resonator (Bruker EN4118X-MD-4-W1). Samples were maintained at 50 K using liquid helium in an Oxford CF-935 cryostat. Field-swept electron spin echos (ESE) were recorded using a 2-pulse ESE sequence while ESE-ENDOR experiments were carried out using Davies three-pulse sequence π-T-$\pi/2$-τ-π-echo with a selective rf pulse of variable frequency applied during time T. The pulse length used were 128 and 256 ns for $\pi/2$ and π respectively, and 10 μs for π-rf pulse. ENDOR data was processed and simulated using the EasySpin package (free download from http://www.easyspin.org/ web page).

Acknowledgements

We thank EaStChem and the EPSRC (UK Basic Technology Programme grant GR/S85726/01) for financial assistance. We also acknowledge financial support from MIUR, Italy (2008 PRIN funds for "Properties and reactivity of free radicals in complex environments and their role in oxidative processes and in organic synthesis").

References

1 S. Bräse, D. Gil, K. Knepper and V. Zimmermann, *Angew. Chem.*, 2005, **117**, 5320; S. Bräse, D. Gil, K. Knepper and V. Zimmermann, *Angew. Chem., Int. Ed.*, 2005, **44**, 5188.
2 M. Minozzi, D. Nanni and P. Spagnolo, *Chem.–Eur. J.*, 2009, **15**, 7830 and references therein.
3 (*a*) L. Benati, P. C. Montevecchi and P. Spagnolo, *Tetrahedron Lett.*, 1978, **19**, 815; (*b*) L. Benati and P. C. Montevecchi, *J. Org. Chem.*, 1981, **46**, 4570; (*c*) S. Kim, G. H. Joe and J. Y. Do, *J. Am. Chem. Soc.*, 1994, **116**, 5521.
4 (*a*) G. Bencivenni, T. Lanza, R. Leardini, M. Minozzi, D. Nanni, P. Spagnolo and G. Zanardi, *J. Org. Chem.*, 2008, **73**, 4721; (*b*) T. Lanza, R. Leardini, M. Minozzi, D. Nanni, P. Spagnolo and G. Zanardi, *Angew. Chem., Int. Ed.*, 2008, **47**, 9439.
5 (*a*) P. A. Baguley and J. C. Walton, *Angew. Chem., Int. Ed.*, 1998, **37**, 3072; (*b*) A. Studer and S. Amrein, *Synthesis*, 2002, 835; (*c*) V. Darmency and P. Renaud, *Top. Curr. Chem.*, 2006, **263**, 71.
6 (*a*) T. Miyai, K. Inoue, M. Yasuda, I. Shibata and A. Baba, *Tetrahedron Lett.*, 1998, **39**, 1929; (*b*) K. Inoue, A. Sawada, I. Shibata and A. Baba, *Tetrahedron Lett.*, 2001, **42**, 4661; (*c*) S. Mikami, K. Fujita, T. Nakamura, H. Yorimitsu, H. Shinokubo, S. Matsubara and K. Oshima, *Org. Lett.*, 2001, **3**, 1853; (*d*) K. Inoue, A. Sawada, I. Shibata and A. Baba, *J. Am. Chem. Soc.*, 2002, **124**, 906; (*e*) K. Takami, H. Yorimitsu and K. Oshima, *Org. Lett.*, 2002, **4**, 2993; (*f*) S.-I. Usugi, T. Tsuritani, H. Yorimitsu, H. Shinokubo and K. Oshima, *Bull. Chem. Soc. Jpn.*, 2002, **75**, 841; (*g*) K. Takami, S. Mikami, H. Yorimitsu, H. Shinokubo and K. Oshima, *Tetrahedron*, 2003, **59**, 6627; (*h*) K. Takami, S. Mikami, H. Yorimitsu, H. Shinokubo and K. Oshima, *J. Org. Chem.*, 2003, **68**, 6627; (*i*) N. Hayashi, I. Shibata and A. Baba, *Org. Lett.*, 2004, **6**, 4981; (*j*) K. Takami, H. Yorimitsu and K. Oshima, *Org. Lett.*, 2004, **6**, 4555; (*k*) N. Hayashi, I. Shibata and A. Baba, *Org. Lett.*, 2005, **7**, 3093; (*l*) K. Takami, S. Usugi, H. Yorimitsu and K. Oshima, *Synthesis*, 2005, **5**, 824; (*m*) N. Hayashi, H. Honda, M. Yasuda, I. Shibata and A. Baba, *Org. Lett.*, 2006, **8**, 4553; For recent general reviews on use of Group 13 organometallic compounds in organic synthesis, see: (*n*) V. Nair, S. Ros, C. N. Jayan and B. S. Pillai, *Tetrahedron*, 2004, **60**, 1959; (*o*) S. Araki and T. Hirashita, in *Comprehensive Organometallic Chemistry III*, 2007, vol. 9, pp. 649–751; (*p*) M. Yamaguchi and Y. Nishimura, *Chem. Commun.*, 2008, 35; (*q*) *Main Group Metals in Organic Synthesis*, H. Yamamoto and K. Oshima, ed., Wiley-VCH, Weinheim, 2004.
7 (*a*) L. Benati, G. Bencivenni, R. Leardini, D. Nanni, M. Minozzi, P. Spagnolo, R. Scialpi and G. Zanardi, *Org. Lett.*, 2006, **8**, 2499; (*b*) G. Bencivenni, T. Lanza, M. Minozzi, D. Nanni, P. Spagnolo and G. Zanardi, *Org. Biomol. Chem.*, 2010, **8**, 3444.
8 As far as we know, the only example of reaction between an azide and a Group 13 metal trihalide was reported in 1987 by Takeuchi *et al.* (H. Takeuchi, M. Maeda, M. Mitani and K. Koyama, *J. Chem. Soc., Perkin Trans. 1*, 1987, 57), who noted that aromatic azides, when treated in aromatic solvents in the presence of $AlCl_3$, give rise to a decomposition reaction entailing formation of extremely reactive N-containing species able to give aromatic substitution reactions. He suggested that those species were $AlCl_3$-complexed arylnitrenes ensuing from aryl azide–$AlCl_3$ complexes. Takeuchi also marginally observed that by mixing the aryl azide and $AlCl_3$ in CH_2Cl_2 at 243 K a strong blue colour developed; this colour faded completely, with concomitant nitrogen gas evolution, when the solution was warmed to 273 K. However, no product analysis of the resulting mixture was carried out and no other mechanistic or synthetic data were subsequently obtained about Lewis acid-catalysed decompositions of azides.
9 (*a*) A. R. Forrester, J. M. Hay and R. H. Thomson, In *Organic Chemistry of Stable Free Radicals*, Academic Press, New York, 1968, pp. 254; (*b*) R. Male and R. D. Allendorfer, *J. Phys. Chem.*, 1988, **92**, 6237.
10 (*a*) J. F. Wolf, C. E. Forbes, S. Gould and L. W. Shacklette, *J. Electrochem. Soc.*, 1989, **136**, 2887; (*b*) M. M. Wienk and R. A. Janssen, *J. Am. Chem. Soc.*, 1996, **118**, 10626.
11 A. Petr and L. Dunsch, *J. Phys. Chem.*, 1996, **100**, 4867.
12 Intense colours were also observed by two-electron oxidation of *Variamine blue* in aqueous media with oxidising agents such as Ce(IV), Fe(III), I_2, and Tl(III); see, for example: T. Imamura and M. Fujimoto, *Bull. Chem. Soc. Jpn.*, 1972, **45**, 442–444.
13 ESI analysis also showed another product with mass 243 amu, which could be related to some unidentified intermediate where loss of the methoxy group has still to occur.
14 Gallium trichloride also gives rise to a peak for $GaCl_4^-$. Our conclusion remained tentative because the $GaCl_4^-$ ion could have come from residual reactant.
15 (*a*) I. Streeter, A. J. Wain, M. Thompson and R. G. Compton, *J. Phys. Chem.*, 2005, **109**, 12636; (*b*) L. Omelka, S. Ondrasova, L. Dunsch, A. Petr and A. Stasko, *Monatsh. Chem.*, 2001, **132**, 597.
16 L. Erdey, T. Mesiel, B. Mohos and F. Tüdös, *Talanta*, 1967, **14**, 1477.
17 S. Stoll, B. Epel, S. Vega and D. Goldfard, *J. Chem. Phys.*, 2007, **127**, 164511.
18 *Gaussian 03, Revision A.1*, M. J. Frisch, *et al.*, Gaussian, Inc., Pittsburgh PA, 2003 (see ESI for full reference).
19 For the B3LYP/EPR-iii//B3LYP/6-31G(d) basis set, see: V. Barone, In *Recent Advances in Density Functional Theory*, D. P. Chong, Ed.; World Scientific Publishing Co., Singapore, 1996.
20 For further mechanistic studies see: (*a*) A. Petr and L. Dunsch, *J. Electroanal. Chem.*, 1996, **419**, 55; (*b*) P. Simon, G. Farsang and C. Amatore, *J. Electroanal. Chem.*, 1997, **435**, 65; (*c*) M. Goto, K. Otsuka, X. Chen, Y. Tao and M. Oyama, *J. Phys. Chem. A*, 2004, **108**, 3980.

